Stereochemical Investigation of Macrocyclic Bisbibenzyls with a Stereogenic Center at One of the Ethylene Bridges

by **Chun-Feng Xie**[a]), **Rong-Xiu Zhu**[b]), **Jian-Bo Qu**[a]), **Li-Ning Wang**[a]), **Dong-Xiao Guo**[a]), **Wen-Tao Yu**[c]), **Cheng-Bu Liu**[b]), and **Hong-Xiang Lou***[a])

[a]) Department of Natural Products Chemistry, School of Pharmaceutical Sciences, Shandong University, No. 44 West Wenhua Road, Jinan 250012, P. R. China (phone: +86-531-8382012; fax: +86-531-8382019; e-mail: louhongxiang@sdu.edu.cn)

[b]) Institute of Theoretical Chemistry, School of Chemistry and Chemical Engineering, Shandong University, No. 27 South Shanda Road, Jinan 250100, P. R. China

[c]) State Key Laboratory of Crystal Materials, Shandong University, No. 27 South Shanda Road, Jinan 250100, P. R. China

7′-Hydroxyriccardin C (**1**) and marchantin E (**2**), two macrocyclic bisbibenzyls with a stereogenic center at the ethylene bridge from Chinese liverworts, were investigated stereochemically. Compound **1** was found to be optically active and occurred as a pair of dynamically interchangeable atropisomers at room temperature due to the low barrier of rotation around the biaryl bond, while **2** was a racemic mixture, which was successfully resolved by chiral HPLC into two enantiomers. Their absolute configurations were unequivocally assigned by analysis of temperature-dependent NMR spectra, X-ray crystallographic diffraction, and comparison of experimental and calculated ECD data.

Introduction. – Macrocyclic bisbibenzyls are naturally occurring stilbenoids found mainly in liverwort species [1–3]. Up to now, more than 80 cyclic bisbibenzyls have been isolated from liverworts, and riccardin C is the only example isolated also from a non-liverwort source, *Primula macrocalyx* [4]. Macrocyclic bisbibenzyls are proposed to be biosynthesized from two units of lunularin by phenolic oxidative coupling [5] or from two units of lunularic acid catalyzed by cytochrome P-450 enzymes [6], resulting in either C–C (biaryl) or C–O–C (diphenyl ether) linkages. These compounds have been the focus of much attention because of their broad spectrum of biological activities since their first isolation [7][8]. Total syntheses of several biologically interesting cyclic bisbibenzyls have been achieved *via Wittig*, *Stille–Kelly*, or *Suzuki–Miyaura* reaction [9–13].

Macrocyclic bisbibenzyls have emerged as a new class of '*stereochemically intriguing molecules*' for their planar and axial chirality due to the presence of strained heterocyclic structures. The configurations of macrocyclic bisbibenzyls such as isoplagiochins and bazzanines bearing two biaryl axes [14][15], of diaryl ether-biphenyl type bisbibenzyls such as riccardin D, isoriccardin C, isoplagiochin B, and dihydroisoplagiochin B [16][17], and of dihydrophenanthrene–bibenzyl derivative (+)-cavicularin [18] have been investigated. However, when the ethylene bridge was asymmetrically substituted, determination of the absolute configuration became more complicated.

In our ongoing research of biologically active compounds from the Chinese liverworts [19][20], 7′-hydroxyriccardin C (**1**) and marchantin E (**2**), two macrocyclic

bisbibenzyls with a stereogenic center emerging from an OH- or a MeO-substituted ethylene bridge, were isolated. In this article, we report their absolute configuration determination by analysis of temperature-dependent NMR spectra, X-ray crystallographic diffraction, and comparison between experimental and calculated ECD data.

Result and Discussion. – *Structure Elucidation of Compound* **1**. 7′-Hydroxyriccardin C (**1**), a new riccardin C derivative with a stereogenic center at the ethylene bridge, was isolated from the liverwort *Asterella angusta*. It was obtained as colorless needles with the molecular formula $C_{28}H_{24}O_5$ (*m/z* 440.1611 (M^+; calc. 440.1624)) deduced from high-resolution electron impact mass spectrometry (HR-EI-MS). The ESI-MS/MS product profile of **1** showed characteristic fragment-ion peaks at *m/z* 197, 211, 213, 223, and 237, which indicated the presence of a bisbibenzyl skeleton [21][22]. In the ^{1}H-NMR spectrum of **1** recorded at room temperature in (D_6)acetone, all signals of the H-atoms were broadened except those of the aromatic OH H-atoms. To further explore this phenomenon, variable-temperature ^{1}H-NMR experiments were performed (*Fig. 1*). Spectra were recorded at $-5°$, 25°, and 80° ((D_6)acetone for $-5°$ and 25°; (D_6)DMSO for 80°), respectively. The presence of broad signals was the most noteworthy feature at 25°. The coalescence point was reached as the temperature increased to 80°. Duplication of signals was clearly observed at $-5°$, indicating the occurrence of two atropisomers at low temperature. In the ^{1}H-NMR at 80° in

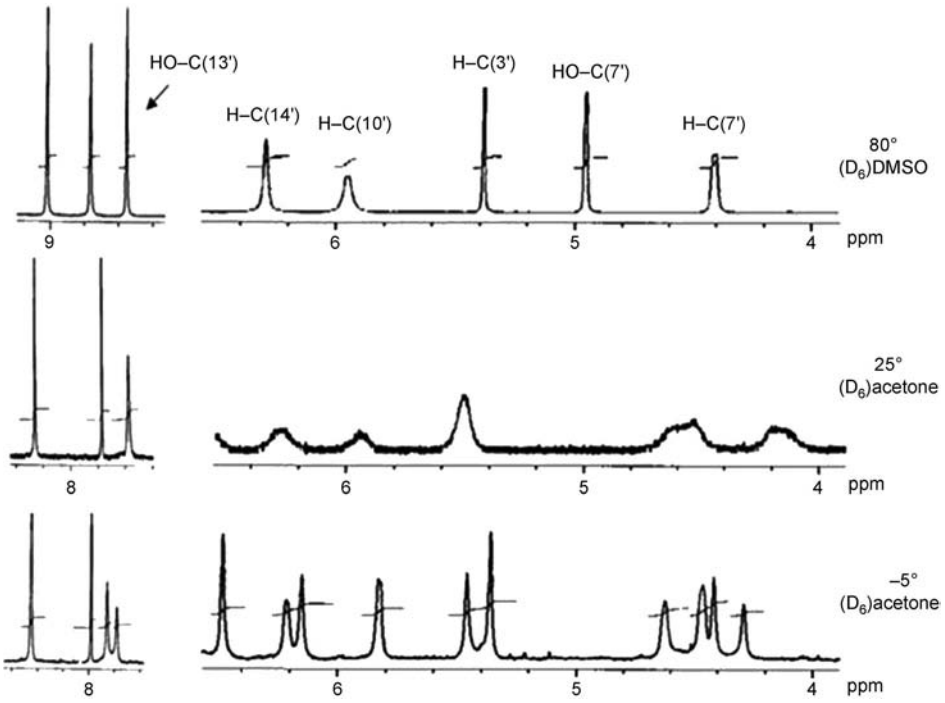

Fig. 1. *Partial dynamic ^{1}H-NMR spectra of compound* **1**

(D_6)DMSO (*Table*), signals corresponding to three benzylic CH_2 groups, one benzylic CH group, and four benzene rings indicated a typical bisbibenzyl structure [2]. The signals at δ(H) 6.65 and 6.75–6.79 were assigned to a 1,4-disubstituted benzene ring (ring *A*), while the three signals at δ(H) 6.61, 6.79, and 6.81 indicated the presence of a 1,2,5-trisubstituted benzene ring (ring *B*). The signals at δ(H) 5.37, 6.93, 6.83, 5.93, 6.64, and 6.27 indicated the presence of two 1,2,4-trisubstituted benzene rings (rings *C* and *D*). The linkages of the rings *A* and *B via* fragment CH_2(7)–CH_2(8), and of the rings *C* and *D via* OH–CH(7′)–CH_2(8′) were confirmed by the long-range correlation of H–C(10) with C(8) and by the NMR chemical-shift values (*Fig. 2*). The highfield-shifted characteristic resonance for H–C(3′) (δ(H) 5.37) suggested a diphenyl ether linkage between C(1) and C(2′) [23]. Accordingly, compound **1** was unequivocally identified as 7′-hydroxyriccardin C, and the structure was confirmed by X-ray diffraction studies (*Fig. 3*).

Table. *^{1}H- and ^{13}C-NMR* (at 600 and 150 MHz, resp.) *Data of Compound* **1** *in (D_6)DMSO* (80°)[a])

Position	δ(H)	δ(C)	Position	δ(H)	δ(C)
1		153.0	1′		144.6
2	6.65 (*d*, *J* = 9.0)	121.3	2′		146.1
3	6.75–6.79 (*m*)	128.7	3′	5.37 (br. *s*)	114.9
4		138.8	4′		135.3
5	6.75–6.79 (*m*)	128.7	5′	6.93 (*d*, *J* = 7.2)	117.9
6	6.65 (*d*, *J* = 9.0)	121.3	6′	6.83 (*d*, *J* = 9.0)	115.7
7	2.71–2.74 (*m*)	37.2	7′	4.43 (br. *s*)	73.3
8	2.86–2.88 (*m*)	34.6	8′	2.80 (*d*, *J* = 12.0), 2.07 (br. *s*)	46.1
9		142.5	9′		136.2
10	6.79 (*d*, *J* = 2.4)	115.9	10′	5.93 (br. *s*)	120.2
11		156.2	11′	6.64 (*d*, *J* = 7.8)	131.4
12	6.61 (*dd*, *J* = 2.4, 8.4)	112.6	12′		125.5
13	6.81 (*d*, *J* = 8.4)	131.8	13′		152.9
14		129.1	14′	6.27 (br. *s*)	117.0

[a]) All assignments are based the X-ray diffraction experiment, 2D-NMR data, and spectral comparison with literature data [2].

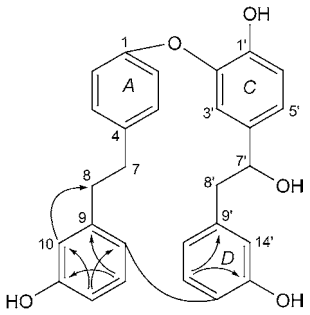

Fig. 2. *Key long-range correlations from the HMBC spectrum of compound* **1**

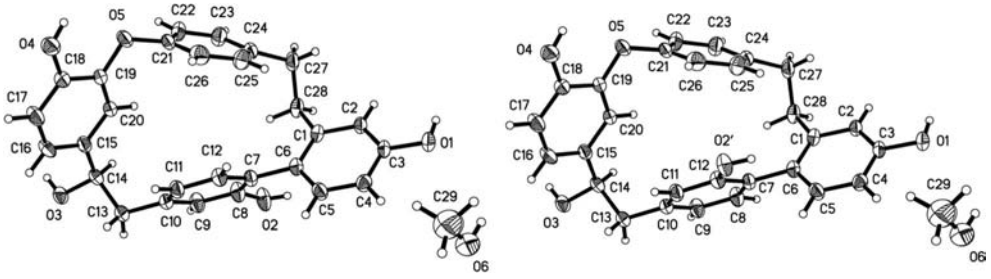

Fig. 3. *Single-crystal X-ray structure of* **1** *with its two atropisomers*

Configuration Assignment. Compound **1** had a $[\alpha]_D^{20}$ value of -21.0 ($c = 0.2$, MeOH), and its ECD spectrum exhibited a strong negative *Cotton* effect at 196 and a positive *Cotton* effect at 223 nm. Different from riccardin C [2][24], the presence of one stereogenic center at the ethylene bridge and the hindrance of rotation around the biaryl axis due to the *ortho*-substituted OH groups led to the occurrence of two diastereoisomeric and thermally interconvertable atropisomers as revealed by temperature-dependent ^{1}H-NMR spectra. The X-ray diffraction analysis also confirmed this observation, since the crystal structure of **1** contained two stereoisomers with different orientations of the OH group at C(13′) in ring *D*. Attempts to resolve the individual atropisomers were unsuccessful as indicated by HPLC/ECD analysis at room temperature.

To determine the absolute configuration of **1**, four stable conformers were identified by using DFT calculations (*Fig. 4*). We predicted the ECD spectra of **1** by applying TDDFT methodology with the Gaussian 03 program package. The ECD spectra indicating weighted (*R*) configurations for isomer 1 and isomer 3, and weighted (*S*)-configurations for isomer 2 and isomer 4 are shown in *Fig. 5*, together with the experimental spectrum of **1**. Comparison of the calculated ECD spectrum with the experimental one gave a good match with the (*R*)-configuration at C(7′), whereas the theoretical spectrum that predicted the (7′*S*)-configuration gave an almost opposite ECD curve. The structure of **1** was finally established as (7′*R*)-hydroxyriccardin C.

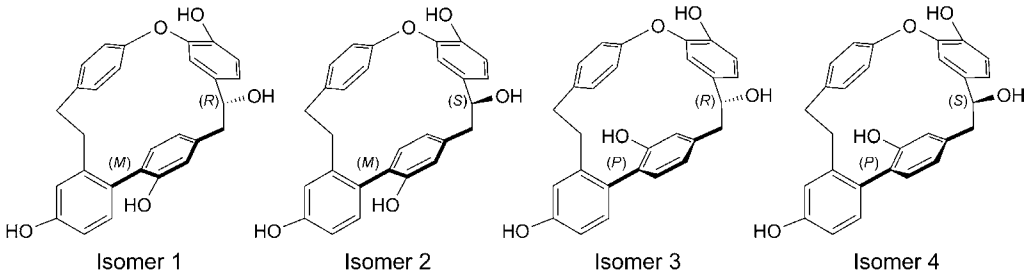

Fig. 4. *Four possible stereoisomers of* **1**

In the case of marchantin E (**2**), no atropisomers were found for the enlarged cyclic structure of the double 'C–O–C' linkages between two bibenzyls, which was confirmed by its temperature-dependent ^{1}H-NMR spectra. But it was unexpected that compound

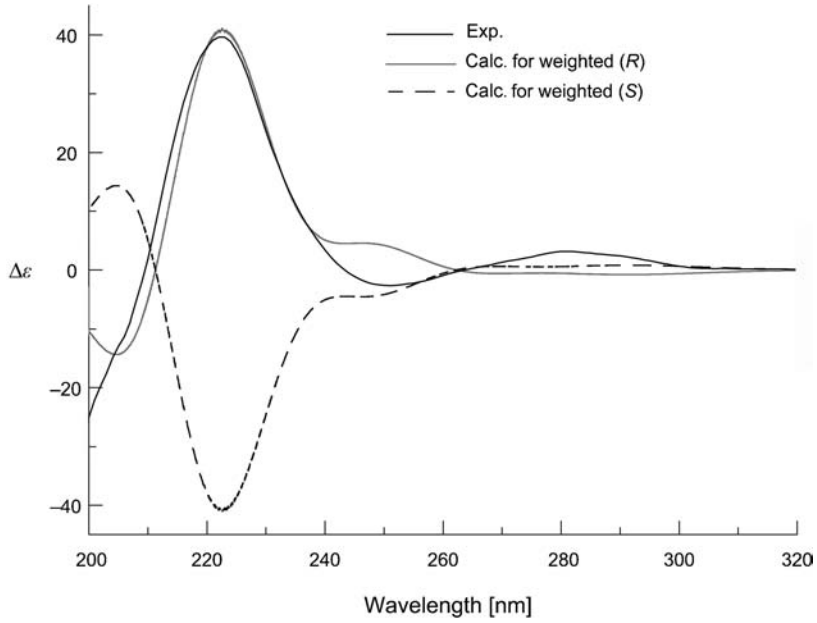

Fig. 5. *Assignment of the absolute configuration of* **1** *by comparison of the experimental ECD spectrum* (black line) *with those calculated for weighted (*R*)* (grey line) *and (*S*)* (dash line)

2 was isolated from *Marchantia polymorpha* as a racemate due to the occurrence of a stereogenic center at the ethylene bridge. To investigate the possible occurrence of enantiomers and to determine their stereochemical properties, resolution by HPLC on a chiral stationary phase was carried out. A perfect baseline separation of two peaks (**2a** for peak *A* and **2b** for peak *B*) at room temperature was achieved by using a *Chiralpak AS-H* column (*Daicel*) with i-PrOH/hexane 7:3 as eluant. That the two LC-UV peaks observed (*Fig. 6,a*) indeed corresponded to the respective enantiomers of **2** was clearly verified by on-line CD recording (*Fig. 6,b*). Integration of the signals obtained gave a 1:1 enantiomeric ratio, demonstrating the fully racemic character of **2**. Accordingly, the optical activity of both enantiomers **2a** and **2b** apparently originated from the stereogenic center C(7′).

Again, a quantum-chemical ECD calculation was performed to attribute the respective absolute configurations to the corresponding enantiomers of **2**. Comparison of the calculated results with the experimental spectra of **2a** and **2b** revealed good agreements between (*R*)-**2** and **2a** (*Fig. 7*, left) and between (*S*)-**2** and **2b** (*Fig. 7*, right).

Conclusions. – The steric hindrance caused by the *ortho*-substitution at the biaryl axis in bisbibenzyl structures result in atropisomeric configuration and optical activity [14][16]. The presence of a further stereogenic center at the ethylene bridge after hydroxylation or methoxylation complicates the configuration of these macrocyclic bisbibenzyl derivatives. For compound **1**, a ricardin-type bisbibenzyl, the optical property was an additive result of a stereogenic center and the biaryl axis. Compound **1**

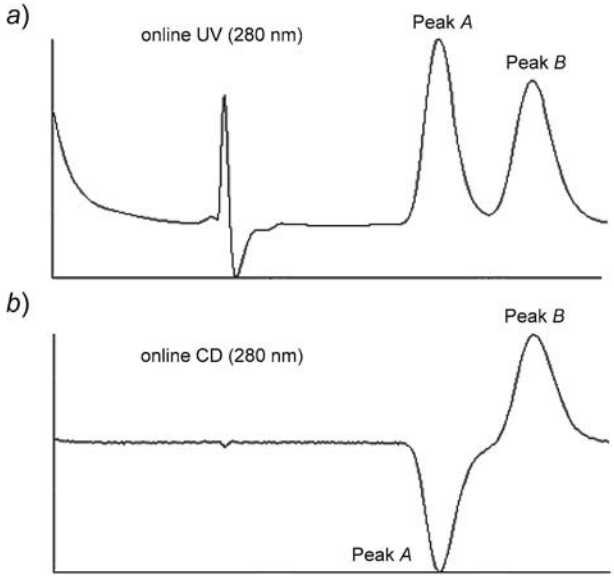

Fig. 6. a) *LC-UV and* b) *LC-CD chromatograms of marchantin E from* M. polymorpha

occurs as an atropisomeric mixture as revealed by the X-ray crystallography, and the atropisomers are thermally interconvertable as detected by variable-temperature ^{1}H-NMR. Taking the (*M*)- and (*P*)-configurations of the biaryl linkage into consideration, quantum-chemical ECD calculations led to the determination of the absolute configuration at C(7′) as (*R*).

Compound **2** was found to be a racemic mixture. The ring in this marchantin-type structure was enlarged because of the double 'C–O–C' linkages between two bibenzyl units. The planar and axial chirality no longer existed due to the rapid interconversion between different configurations. The stereogenic centers at the ethylene bridge contribute to the whole optical activity of the molecule. Again, based on quantum-chemical ECD calculations, the (*R*)- and (*S*)-enantiomers of **2** were unequivocally determined. As it has been reported that marchantin D could be converted to marchantin E when dissolved in MeOH [25], the two enantiomers of the racemic mixture of marchantin E (**2**) were possibly formed by methoxylation of marchantin D during isolation.

In conclusion, our results indicate that nature really does not produce macrocyclic bisbibenzyls in an enantiomerically pure form [14][15]. Additionally, this investigation of riccardin- and marchantin-type bisbibenzyl configurations should thus contribute significantly to the assessment of the absolute configurations of similar bisbibenzyls.

This work was supported by the *National Natural Science Foundation of China* (No. 30925038 and No. 30730109). We express our sincere gratitude to Prof. *Qian Gao*, Shenyang Institute of Applied Ecology, for plant identification.

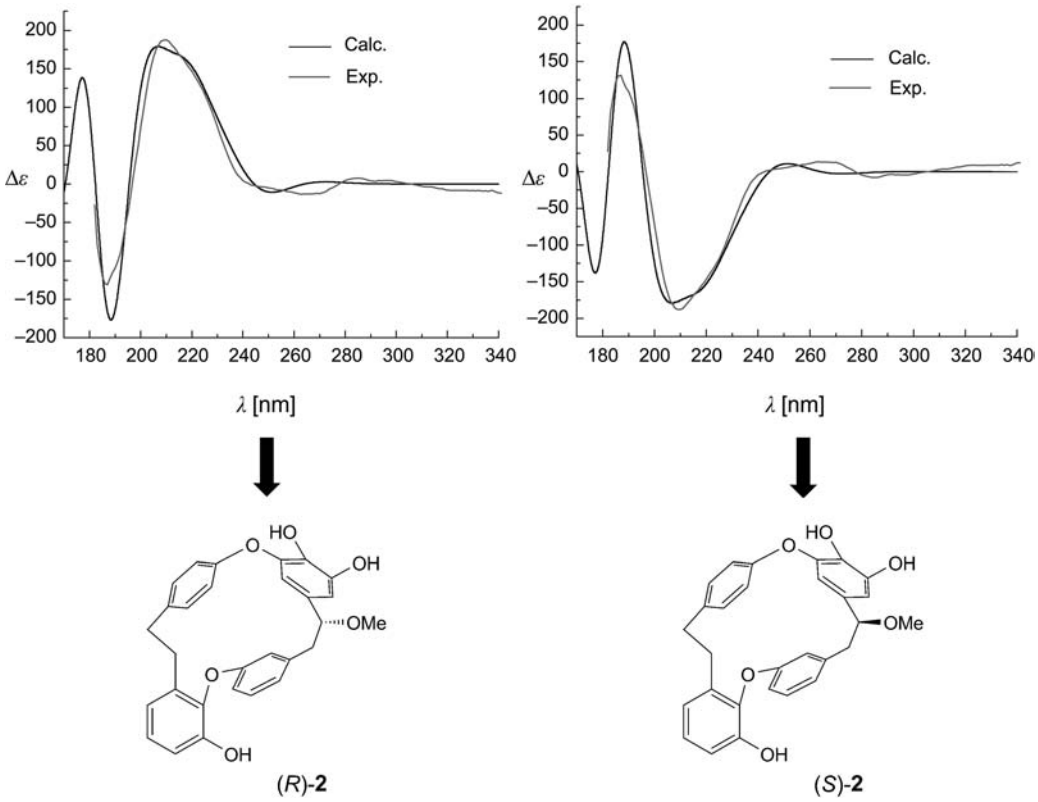

Fig. 7. *Assignment of the absolute configuration of* **2** *to peaks* A *and* B *as (*R*) and (*S*), respectively, by comparison of their experimental ECD spectra with those calculated for (*R*)- and (*S*)-marchantin E* (**2**)

Experimental Part

General. Chromatographic grade hexane and i-PrOH were used for HPLC (*Siyou Chemical Factory*, Tianjin, P. R. China). Other reagents were of anal. grade (*Laiyang Chemical Factory*, Shandong, P. R. China). Column chromatography (CC): silica gel (SiO_2; *Qingdao Haiyang Chemical Plant*, Qingdao, P. R. China; 200–300 mesh) and *Sephadex LH-20* (*Pharmacia Biotek*, Denmark). Off-line ECD spectra: *Chirascan* circular dichroism spectrometer. The HPLC/ECD coupling system consisted of a *JASCO* pump *PU2080* with *Rheodyne* 20 µl sample loops, an ECD *2095* detector, and *Borwin* chromatographic software (*JASCO*, *Tokyo*, Japan). M.p.: *X-6* micro-melting point apparatus (*Beijing TECH Instrument Co., Ltd.*, P. R. China); uncorrected. Optical rotations: *Perkin–Elmer 241 MC* polarimeter. UV Spectra: *Shimadzu UV-2450* spectrophotometer; λ_{max} (log ε) in nm. IR Spectra: *Thermo-Nicolet 670* spectrophotometer; $\tilde{\nu}$ in cm^{-1}. NMR Spectra: *Bruker Avance DRX-600* spectrometer operating at 600 (^1H) or 150 (^{13}C) MHz; δ in ppm rel. to Me_4Si as internal standard, J in Hz. 2D-NMR Spectra: recorded using standard pulse programs and acquisition parameters. ESI-MS: *API 4000* triple-stage quadrupole instrument; in *m*/*z*. HR-EI-MS: *LTQ-Orbitrap* mass spectrometer, in *m*/*z* (rel. %).

Plant Material. A. angusta (STEPH.) PANDE was collected from Mount Gui-cheng, Sichuan Province, P. R. China, and identified by Prof. *Qian Gao*, Shenyang Institute of Applied Ecology, Chinese Academy of Sciences. The voucher specimen (No. 20040627) was deposited with the Department of Natural Products Chemistry, School of Pharmaceutical Sciences, Shandong University.

Extraction and Isolation. Air-dried and powdered *A. angusta* (2.5 kg) was extracted with 95% EtOH (6 l) by heating under reflux for 2.5 h. The process was repeated three times, and the combined extract was evaporated *in vacuo*, yielding 78 g of crude extract. The crude extract was suspended in H_2O (500 ml) and partitioned sequentially three times with Et_2O (250 ml) and BuOH (250 ml). The Et_2O extract (32 g) was fractionated by CC (SiO_2; petroleum ether (PE)/acetone gradient). Seven fractions were obtained. Purification of *Fr. 7* (3.7 g; PE/acetone 7:3) on *Sephadex LH-20* yielded compound **1** (10 mg; recrystallized from MeOH).

Compound **2** was isolated previously from Chinese liverwort *Marchantia polymorpha* in our laboratory, and its structure was established as marchantin E by MS and NMR [26].

Stereoisomer Analysis by HPLC-CD Coupling. The chiral stationary phase used for separation of stereoisomers was *Chiralpak AS-H* (250 mm × 4.6 mm, *Daicel*, Tokyo, Japan). For compound **1**, the mobile phase was a i-PrOH/hexane mixture. The flow rate was 0.5 ml/min at r.t. UV and CD detectors were set at 280 nm. Compound **2** was resolved by means of HPLC with i-PrOH/hexane 3:7 (flow rate 0.5 ml/min) using the chiral column to yield two fractions, **2a** (t_R 17 min) and **2b** (t_R 23 min). The detection was carried out at 280 nm.

7′-Hydroxyriccardin C (**1**). Colorless needles (MeOH). M.p. 220–221°. $[\alpha]_D^{20} = -21.0$ ($c = 0.2$, MeOH). UV (MeOH): 210 (4.75), 274 (3.60). CD: $[\theta]_{223}$ 6.6×10^4, $[\theta]_{251}$ -4.5×10^3, $[\theta]_{281}$ 5.3×10^3, $[\theta]_{210, 243, 264}$ 0. IR (KBr): 3473, 1609, 1476, 1300. ^{1}H- and ^{13}C-NMR: *Table*. ESI-MS (pos.): 423 ($[M + H - H_2O]^+$). HR-EI-MS: 440.1611 (M^+, $C_{28}H_{24}O_5^+$; calc. 440.1624).

X-Ray Crystallographic Analysis of **1**[1]). Single crystals suitable for X-ray-analysis were obtained by recrystallization from MeOH. A colorless platelet crystal with approximate dimensions of 0.32 mm × 0.21 mm × 0.12 mm was used for analysis. All measurements were made on a *Bruker APEX2 CCD* area-detector diffractometer using graphite monochromated MoK_α radiation ($\lambda = 0.71073$ Å) at 293 K and operating in ϕ-ω scan mode. Crystallographic data: $C_{28}H_{24}O_5 \cdot$MeOH, M_r 472.52, monoclinic, space group P2(1), $a = 11.8008(6)$ Å, $b = 8.9305(6)$ Å, $c = 12.2125(8)$ Å, $\beta = 111.241(3)°$, $V = 1199.60(13)$ Å^3, $Z = 2$, $D_{calc.} = 1.305$ Mg/m^3, $F(000) = 498$ and μ(MoK_α) = 0.091 mm^{-1}. Cell refinement and data reduction: APEX2 Software Suite [27]. Program used to refine structure: SHELXL-97 [28]; refinement on F^2, full-matrix least-squares calculations. All non-H-atoms were refined anisotropically, and all H-atoms were placed in geometrically calculated positions and refined as riding atoms with the relative isotropic parameters. One lattice MeOH molecule was contained in the structure. 6203 reflections (2928 unique, $R_{int} = 0.0242$) were collected in the range $\theta = 2.90$ to 27.53° and index ranges $12 \geq h \geq -15$, $7 \geq k \geq -11$, $15 \geq I \geq -15$. The final stage converged to $R_1 = 0.0453$ ($wR_2 = 0.1179$) for 2928 observed reflections (with $I > 2\sigma(I)$) and 333 variable parameters, $R_1 = 0.0617$ ($wR_2 = 0.1309$) for all unique reflections, and Goodness-of-fit 1.008.

*(*R*)-Marchantin E* (**2a**). White amorphous solid. $[\alpha]_D^{20} = +45.0$ ($c = 0.07$, MeOH). CD: $[\theta]_{187}$ -6.5×10^2, $[\theta]_{210}$ 9.4×10^2, $[\theta]_{267}$ -65.9, $[\theta]_{197, 143}$ 0.

*(*S*)-Marchantin E* (**2b**). White amorphous solid. $[\alpha]_D^{20} = -89.0$ ($c = 0.10$, MeOH). CD: $[\theta]_{195}$ 6.4×10^2, $[\theta]_{217}$ -9.3×10^2, $[\theta]_{289}$ 88.7, $[\theta]_{205, 251}$ 0.

Computations. The calculations were conducted by using density-functional theory (DFT) as implemented in the Gaussian 03 [29]. We choose the semiempirical AM1 method and a DFT approach (B3LYP/6-31G*) to scan the potential energy surface (PES). Ground-state geometries were optimized at the B3LYP/6-31G* level, and frequency calculations were carried out to confirm these minima and to calculate free energies at 298.15 K. Electronic excitation energies and rotational strengths in gas phase and in MeOH were calculated using TDDFT at the same level both in velocity and in length formalism for the first 30 states for **1** and 90 states for **2**. The rotatory strengths were summed and energetically weighted according to the *Boltzmann* statistics. Then, the CD curves were simulated by using the Gaussian function [30]:

---

[1]) Details of crystallographic data (excluding structural factors) for the structural analysis have been deposited with the *Cambridge Crystallographic Data Centre* as supplementary publication No. CCDC-631368. Copies of the data can be obtained free of charge on application to *CCDC*, 12 Union Road, Cambridge CB21EZ, UK (fax: +44-1223-336033; e-mail: deposit@ccdc.cam.ac.uk).

$$\varepsilon(E) = \frac{1}{2.296 \times 10^{-39}} \frac{1}{\sqrt{\sigma}} \times \sum_i E_i R_i e^{-[(E-E_i)/\sigma]^2}$$

where σ is half the band width at $1/e$ height, and ΔE_i and R_i are the excitation energies and rotatory strengths for transition i, resp. Here, a value of $\sigma = 0.4$ eV was used for compounds **1** and **2**.

REFERENCES

[1] G. M. Keserű, M. Nógrádi, *Nat. Prod. Rep.* **1995**, *12*, 69.
[2] Y. Asakawa, M. Toyota, M. Tori, T. Hashimoto, *Spectroscopy* **2000**, *14*, 149.
[3] Y. Asakawa, M. Toyota, T. Hashimoto, M. Tori, F. Nagashima, L. Harinantenaina, *Heterocycles* **2008**, *76*, 99.
[4] Y. S. Kosenkova, M. P. Polovinka, N. I. Komarova, D. V. Korchagina, N. Y. Kurochkina, V. A. Cheremushkina, N. F. Salakhutdinov, *Chem. Nat. Compd.* **2008**, *43*, 712.
[5] H. D. Zinsmeister, H. Becker. T. Eicher, *Angew. Chem., Int. Ed.* **1991**, *30*, 130.
[6] S. Friederich, M. Rueffer, Y. Asakawa, M. H. Zenk, *Phytochemistry* **1999**, *52*, 1195.
[7] Y. Asakawa, M. Toyota, R. Matsuda, K. Takikawa, T. Takemoto, *Phytochemistry* **1983**, *22*, 1413.
[8] Y. Asakawa, M. Toyota, Z. Taira, T. Takemoto, M. Kido, *J. Org. Chem.* **1983**, *48*, 2164.
[9] Y. Fukuyama, H. Yaso, K. Nakamura, M. Kodama, *Tetrahedron Lett*. **1999**, *40*, 105.
[10] G. V. López, E. M. Pandolfi, G. A. Seoane, *Synthesis* **2000**, 1403.
[11] T. Esumi, M. Wada, E. Mizushima, N. Sato, M. Kodama, Y. Asakawa, Y. Fukuyama, *Tetrahedron Lett*. **2004**, *45*, 6941.
[12] D. C. Harrowven, T. Woodcock, P. D. Howes, *Angew. Chem., Int. Ed.* **2005**, *44*, 3899.
[13] H. Hioki, N. Shima, K. Kawaguchi, K. Harada, M. Kubo, T. Esumi, T. Nishimaki-Mogami, J.-i. Sawada, T. Hashimoto, Y. Asakawa, Y. Fukuyama, *Bioorg. Med. Chem. Lett*. **2009**, *19*, 738.
[14] G. Bringmann, J. Mühlbacher, M. Reichert, M. Dreyer, J. Kolz, A. Speicher, *J. Am. Chem. Soc.* **2004**, *126*, 9283.
[15] J. M. Scher, J. Zapp, H. Becker, N. Kather, J. Kolz, A. Speicher, M. Dreyer, K. Maksimenka, G. Bringmann, *Tetrahedron* **2004**, *60*, 9877.
[16] L. N. Wang, C. F. Xie, X. S. Zhu, P. H. Fan, H. X. Lou, *J. Asian Nat. Prod. Res.* **2011**, *13*, 312.
[17] H. Morita, Y. Tomizawa, T. Tsuchiya, Y. Hirasawa, T. Hashimoto, Y. Asakawa, *Bioorg. Med. Chem. Lett*. **2009**, *19*, 493.
[18] M. Toyota, T. Yoshida, Y. Kan, S. Takaoka, Y. Asakawa, *Tetrahedron Lett*. **1996**, *37*, 4745.
[19] C. Xie, H. Lou, *Curr. Org. Chem.* **2008**, *12*, 619.
[20] D.-X. Guo, R.-X. Zhu, X.-N. Wang, L.-N. Wang, S.-Q. Wang, Z.-M. Lin, H.-X. Lou, *Org. Lett.* **2010**, *12*, 4404.
[21] H. Guo, J. Xing, C. Xie, J. Qu, Y. Gao, H. Lou, *Rapid Commun. Mass Spectrom*. **2007**, *21*, 1367.
[22] J. Xing, C. Xie, J. Qu, H. Guo, B. Lv, H. Lou, *Rapid Commun. Mass Spectrom*. **2007**, *21*, 2467.
[23] M. Tori, M. Toyota, L. J. Harrison, K. Takikawa, Y. Asakawa, *Tetrahedron Lett*. **1985**, *26*, 4735.
[24] Y. Asakawa, R. Matsuda, *Phytochemistry* **1982**, *21*, 2143.
[25] Y. Asakawa, M. Toyota, F. Nagashima, T. Hashimoto, *Nat. Prod. Commun.* **2008**, *3*, 289.
[26] C. Niu, J.-B. Qu, H.-X. Lou, *Chem. Biodiversity* **2006**, *3*, 34.
[27] APEX II. User Manual, Bruker AXS Inc., 2005.
[28] G. M. Sheldrick, 'SHELXTL, Version 5, Reference Manual', Siemens Energy and Automation, Inc., 1997.
[29] M. J. Frisch, G. W. Trucks, H. B. Schlegel, G. E. Scuseria, M. A. Robb, J. R. Cheeseman, J. A. Montgomery Jr., T. Vreven, K. N. Kudin, J. C. Burant, J. M. Millam, S. S. Iyengar, J. Tomasi, V. Barone, B. Mennucci, M. Cossi, G. Scalmani, N. Rega, G. A. Petersson, H. Nakatsuji, M. Hada, M. Ehara, K. Toyota, R. Fukuda, J. Hasegawa, M. Ishida, T. Nakajima, Y. Honda, O. Kitao, H. Nakai, M. Klene, X. Li, J. E. Knox, H. P. Hratchian, J. B. Cross, V. Bakken, C. Adamo, J. Jaramillo, R. Gomperts, R. E. Stratmann, O. Yazyev, A. J. Austin, R. Cammi, C. Pomelli, J. W. Ochterski, P. Y. Ayala, K. Morokuma, G. A. Voth, P. Salvador, J. J. Dannenberg, V. G. Zakrzewski, S. Dapprich,

A. D. Daniels, M. C. Strain, O. Farkas, D. K. Malick, A. D. Rabuck, K. Raghavachari, J. B. Foresman, J. V. Ortiz, Q. Cui, A. G. Baboul, S. Clifford, J. Cioslowski, B. B. Stefanov, G. Liu, A. Liashenko, P. Piskorz, I. Komaromi, R. L. Martin, D. J. Fox, T. Keith, M. A. Al-Laham, C. Y. Peng, A. Nanayakkara, M. Challacombe, P. M. W. Gill, B. Johnson, W. Chen, M. W. Wong, C. Gonzalez, J. A. Pople, Gaussian03, revision A.1, Gaussian, Inc., Pittsburgh, PA, 2004.

[30] P. J. Stephens, N. Harada, *Chirality* **2010**, *22*, 229.

Received April 27, 2011